Intracellular labile iron pools as direct targets of iron chelators: a fluorescence study of chelator action in living cells

Hava Glickstein, Rinat Ben El, Maya Shvartsman, and Z. Ioav Cabantchik

The primary targets of iron chelators used for treating transfusional iron overload are prevention of iron ingress into tissues and its intracellular scavenging. The present study was aimed at elucidating the capacity of clinically important iron chelators such as deferiprone (DFP), desferrioxamine, and ICL670 to (a) gain direct access to intracellular iron pools of key cells of iron accumulation (macrophages, hepatocytes, and cardiomyocyte cell lines); (b) chelate the labile iron present in discrete cell compartments/organelles; and (c) prevent labile iron involvement in the generation of reactive oxidant species. Chelation of cytosolic and organellar cell iron was visualized dynamically and quantitatively in living cells by fluorescence microscopic imaging of fluorescent metallosensors (used as iron-quenched complexes of calceins) targeted to either cytosol, endosome-lysosomes, or mitochondria. The rate and extent of fluorescence recovery provided an in situ measure of the accessibility of chelators to particular cell sites/organelles. Complementary, fluorogenic redox probes associated with cell compartments enabled identification of chelator-sensitive, localized reactive oxidant production. Our studies indicate that chelation by desferrioxamine is slow and is enhanced in cells with relatively high endocytic activities, while ICL670 and DFP readily enter most cells and efficiently reach the major intracellular sites of iron accumulation. (Blood. 2005;106:3242-3250)

Introduction

Cell damage associated with iron overload has been attributed to the emergence of levels of cell labile iron pools (LIPs) that promote production of reactive oxygen species (ROSs) exceeding cellular defense capacities.[1,2] In thalassemia major, there is an outpouring of catabolic iron that overwhelms the iron-carrying capacity of plasma transferrin and generates redox-active forms[1] that may potentially cause tissue iron overload, damaging vital organs such as heart, liver, and endocrine glands.[3,4] The major objective of iron chelation therapy in transfusional hemosiderosis is the reduction of body iron burden by safe removal of toxic iron from organs and extracellular fluids.[1,3,4] The main chelation target has been iron in the liver, the major organ of pathologic iron accumulation.[1,4-6] Outstanding results have been achieved with deferoxamine (DFO), which is administered via parenteral routes.[5-10] However, despite intensive chelation treatment, siderotic cardiac disease has been the complication responsible for 71% of thalassemic mortality, while infection accounts for only 12% (hepatic [6%], endocrine [3%], or malignancies [3%]).[7-12] A serious factor in treatment outcome has been compliance with the rigorous requirements of daily subcutaneous DFO infusions; therefore, patients who are noncompliant with continuous DFO treatment might die prematurely of cardiac complications. The issue of noncompliance has stimulated the design of alternative, orally effective chelators that would be more convenient for use and thus improve compliance as well as protect hepatic and extrahepatic organs from the deleterious effects of iron overload.[1,5,13,14] This has led to the use of hydroxypyrydin-on deferiprone (DFP or L1) and bishydroxyphenyl thiazole (ICL670 or ICL) as alternatives to DFO.[5,11-13] Hitherto, few studies have dealt with the routes of chelator entry into cells of relevance to iron toxicity and their respective subcellular chelation targets, particularly in iron overload.[15,16]

The present work examines the modes by which the 3 clinically important chelators, DFO, ICL, and DFP, gain access to critical sites of iron accumulation in different cells and how those modes contribute to their chelation capacity. The model cell lines used are rat cardiomyocytes (H9C2), mouse macrophages (J774), and human hepatocytes (HEPG2). The analytical objects used to monitor chelator action are the LIPs,[17-19] which represent the redox active and chelatable forms of iron that are present in the cell cytosol[20-22] and in organelles such as endosome-lysosomes and mitochondria.[16,23] In previous studies, these LIPs were visualized by fluorescent metallosensors targeted principally to 2 cell compartments (cytosol and mitochondria), allowing online monitoring of chelator action in normal and iron-overloaded living cells.[16,18-26] The present study focuses on the ability of chelators to scavenge iron from the different cellular organelles as monitored by fluorescence analysis of living cells (a) that were treated with chelators or (b) in which fluorescence-quenched complexes of iron and sensor were either generated in situ (in the cell) or incorporated (targeted) as preformed complexes into specific cell organelles. The access of test chelators to iron-laden compartments evokes an increase in sensor fluorescence, globally in the cell or locally in cell compartments, as the case might be. For the LIP analysis, we used both fluorescence microscopy imaging methods and high throughput online fluorescence tracing in microplates. Our studies indicate that chelators in clinical or preclinical use have different modes of

From the Department of Biological Chemistry, Alexander Silberman Institute of Life Sciences, Hebrew University of Jerusalem, Jerusalem, Israel.

Submitted February 2, 2005; accepted April 30, 2005. Prepublished online as *Blood* First Edition Paper, July 14, 2005; DOI 10.1182/blood-2005-02-0460.

Supported in part by the European Community 5th Framework QLRT-2001-00444, Novartis (Basel), Apopharm (Toronto), and the Charles E. Smith Center for Psychobiology.

Reprints: Ioav Cabantchik, Department of Biological Chemistry, Institute of Life Sciences, Hebrew University of Jerusalem, Safra Givat Ram Campus, Jerusalem 91904, Israel; e-mail: ioav@cc.huji.ac.il.

The publication costs of this article were defrayed in part by page charge payment. Therefore, and solely to indicate this fact, this article is hereby marked "advertisement" in accordance with 18 U.S.C. section 1734.

access to cell LIPs in different cell types and therefore different efficacies in relieving different cell types from iron overload.

Materials and methods

Materials and cells

Calcein green (CALG), calcein blue (CALB), and their acetomethoxies (AMs) CALG-AM and CALB-AM; dihydrorhodamine 123 (DHR); sulforhodamine; BAPTA ((bis (o-aminophenoxy)-ethane-*N,N,N′,N′*-tetraacetic acid); DTPA (diethylene-triamine-pentaacetic acid); and CDDHCF-DA (2′-7′-Carboxydichlorodihydrofluorescein-diacetate) were procured from Molecular Probes (Eugene, OR). Human serum albumin was from Kamada (Kibbutz Beth Kama, Israel), and, unless specified otherwise, all other chemicals were from Sigma Chemical (St Louis, MO). SIH (salicylaldehyde isonicotynoyl hydrazone) was a gift from Prof Prem Ponka (Montreal, QC); DFP or L1 (1,2-dimethyl-3-hydroxy-4-pyridinone) was from Apopharm (Toronto, ON); and ICL670 (ICL; (4-[3,5-bis(2-hydroxyphenyl)-1,2,4-triazol-1-yl]-benzoic acid) and desferrioxamine (DFO) were from Novartis Pharma (Basel, Switzerland). The cell lines of human hepatoma HepG2, mouse macrophage J774, and cardiomyocyte H9C2 were grown in 5% CO_2 in Dulbecco modified Eagle medium (DMEM) supplemented with 10% fetal calf serum, 4.5 g/L D-glucose, glutamine, and antibiotics (all from Biological Industries, Kibbutz Bet Haemek, Israel). For experimentation, the cells were detached with trypsin-EDTA (ethylenediaminetetraacetic acid), washed with growth medium, and cultured for an additional 24 hours of growth in either 96-well plates (Nunc, Copenhagen, Denmark) or coverslips. The plates were used for tracing fluorescence in a plate reader (Galaxy; BMG-Technologies, Offenburg, Germany or Safire-Tecan, Männedorf, Austria); coverslips were used for fluorescence microscope imaging by laser scanning microscopy (LSM, confocal) system MRC1024 (Biorad, Hemel Hampstead, United Kingdom) or epifluorescence (Zeiss Axiovert 35; Carl Zeiss, Jena, Germany) attached to a Polychrome V image system (Till Photonics, Gräfelfing, Germany).

The samples were inspected with a 60 ×/1.3 objective lens and recorded with a Sensicon PCO modified CCD camera (adapted by Till Photonics, Gräfeling, Germany). Image analysis was performed with Till Photonics software in conjunction with NIM Image J (National Institutes of Health, Bethesda, MD).

Loading CALG or CALB to cytosolic compartment using the respective AM derivatives

Cells were exposed to either CALB-AM 5 μM or CALG-AM 0.25 μM at 37°C for 10 minutes in DMEM containing 10 mM Na-HEPES (*N*-2-hydroxyethylpiperazine-*N′*-2-ethanesulfonic acid) and 1 mg/mL bovine serum albumin (loading medium); cells were washed with 37°C HEPES-buffered saline, pH 7.4 (HBS), and subsequently perfused with either HBS or DMEM-HEPES containing 0.5 mM probenecid (to minimize probe leaking[27]).

Loading CALG-Fe (III) or CALB-Fe (III) (1:1.2) complexes to endosomal compartments (E) via endocytosis

Cells were exposed to either CALG-Fe or CALB-Fe (50-100 μM) in loading medium for 30 minutes at 37°C and washed with HBS as indicated above.

Loading impermeant chelators to the cytosolic (C) compartment as acetomethoxy (AM) precursors

BAPTA was loaded via its AM precursor by incubating the latter (100 μM final) for 20 minutes in DMEM-Hepes at 37°C followed by washing with HBS. The intracellular concentration of DFO, DTPA, and BAPTA attained was determined by lysing cells (grown in 6-well culture plates and loaded with the chelators) with 1% octylglucopyranoside in HBS and assessing the recovery of fluorescence of 100 nM CALG-Fe (excitation, 488 nm; emission, 520 nm).

Measurement of ROS production[28]

Method 1: Cytosolic ROS formation was determined in cells exposed at 37°C to 10 to 20 μM CDCHF-DA-AM (6′-Carboxy-2′,7′-dichlorodihydrofluorescein-diacetate-acetomethoxy ester). The medium consisted of HBS supplemented with 10 mM glucose. The redox-mediated conversion of the nonfluorescent 2′-7′ Carboxy-dichlorodihydrofluorescein-diacetate (CDDHCF-DA) to the fluorescent 2′-7′ Carboxy-dichlorofluorescein-diacetate (CDCF-DA) was measured either in a fluorescence plate reader (excitation, 488 nm; emission, 517 nm) or under the fluorescence microscope (excitation, 488 nm; emission, 517 nm) and analyzed by image analysis programs.

Method 2: Mitochondrial ROS formation was determined in cells exposed at 37°C to 50 μM DHR, which is oxidized intracellularly to rhodamine 123 (R) and analyzed fluorimetrically/microscopically as described (excitation, 488 nm; emission, 517 nm). At the indicated times, ferrous ammonium sulfate (FAS, 2-20 μM), Fe(III)–8 hydroxyquinoline (1:1), Fe-HQ (2-5 μM), H_2O_2 (20-35 μM final), and/or chelator were added, as indicated.

Results

Transition metals can be analyzed by spectroscopic probes that form stable probe-metal complexes and undergo photo-induced electron transfer phenomena,[29] of which the most common is quenching of the fluorescence signal.[20,30] Since some fluorescent probes are susceptible to photobleaching, it is essential to ascertain when quenching events result from specific complex formation.[24] The present work comprised the joint application of 2 related principles of sensing labile iron with fluorescent probes: (1) the probes' capacity to bind iron stoichiometrically and/or serve as an acceptor of redox active iron and thereby undergo a change in fluorescence properties and (2) the ability of a specific iron chelator to prevent or reverse the binding of the probe or suppress iron redox activity.[20,22] The fluorescence probes used, CALG and CALB, quench upon binding of iron at 1:1 and 2:1 to 3:1 stoichiometry, respectively, and regain fluorescence when chelators are added.[19,20] The fluorescein-based CALG has relatively higher quantum efficiency and therefore better sensitivity than the coumarin-based CALB, yet it is considerably more susceptible to photobleaching when exposed to high light intensities such as in fluorescence microscopy. Thus, whereas CALG is better suited for high throughput measurements such as in plate readers with low-intensity illumination, CALB is suitable also for individual cell microscopy measurements.

In order to assess the ability of chelators to bind LIPs in particular cell compartments, we used 2 forms of labile iron as targets of chelation, the resident forms and those introduced by iron overload. In the first (approach A, Table 1), the cells are pretreated with chelator, and subsequently the residual LIPs are analyzed either with fluorescent metallosensors or with markers of redox activity. In the second (approach B), the chelation of LIP is followed online in terms of the ability of a chelator to restore fluorescence of quenched Fe-CALG or Fe-CALB complexes or to block ROS production in a given cell compartment harboring LIPs. These properties of chelators are taken as a measure of their accessibility (ie, membrane permeability) to a given cell compartment and their apparent capacity to bind resident or loaded iron, thereby preventing its involvement in ROS formation. We measure the latter with dihydro-fluorogenic probes that oxidize intracellularly to fluorescent derivatives in the cytosol (when added as AM precursors) or in mitochondria (when added as hydrophobic-cationic probes that accumulate in the mitochondria via their membrane potential). In order to prevent leakage of anionic

Table 1. Experimental approaches used for online fluorescence assessment of labile iron chelation in cell compartments

Approach A: pretreatment by chelators	Approach B: online assessment of chelation	Approach B′: online assessment of chelation
1. Treat cells with chelator	1. Load cells with CAL (± Fe)	1′. Load cells with CDCF or DHR
2. Analyze residual LIP: a. CAL-SIH cytosol b. CDCF (ROS) cytosol c. DHR (ROS) mitochondria	2. Analyze: add chelator and follow fluorescence recovery in cytosol and/or endosomes	2′. Analyze: add H_2O_2 and chelator, and follow ROS formation by fluorescence in cytosol and/or in mitochondria

In approach A, cells are treated first with chelators and subsequently assessed for residual LIP (a) in the cytosol by the calcein (CAL)–based method and/or by (b) the CDDHCF-DA-based method (Fe-dependent H_2O_2-prompted ROS formation) and (c) in mitochondria by the DHR-based method equivalent to that of CDCF.

In approach B, cells are first loaded with probes for LIP ([1] metallosensor or [1′] redox-reporter). In no. 1, one of the calcein (CAL) probes (supplemented or not with Fe), which is targeted to cytosol or endosomes (as CAL-Fe complexes), is used. The cell LIPs comprise resident forms of labile Fe, those induced by adding permeant sources of labile Fe, or those created in endosomes by endocytosis of CAL-Fe complexes. The various LIPs are revealed by chelating the iron complexed to CAL with excess permeant chelators that release the iron-free fluorescent probe in situ. In no. 2′, CDDHCF-DA is loaded into cytosol and DHR into mitochondria, and the labile (redox-active) Fe is revealed in the respective compartment by its involvement in H_2O_2-prompted ROS formation and susceptibility to added chelators.

fluorescent probes from cells, we added probenecid (0.5 mM), an anion transport blocker.[27]

Cytosolic labile iron following different incubation times of cells with chelators

The ability of DFO and the orally active chelators ICL670 and DFP to access cytosolic LIP and scavenge iron was first assessed by approach A, namely by determining the residual LIP following relatively short (0.5 hours) and long (12 hours) incubations with 50 μM chelator. Figure 1 shows representative data obtained with HepG2 cells, but essentially similar results were obtained with J774 and H9C2 cells (not shown). The residual LIP was assessed at the end of the chelation treatment by loading cells with CALB, generated from its AM precursor. CALB distributes homogeneously in the cell interior, though it is partially excluded from the nuclei (Figure 1A). CALB was chosen for studies based on fluorescence microscopy due to its better photostability. The quenched CALB-Fe complexes (representing LIP) were revealed by SIH, a strong permeant chelator that restores fluorescence by removing the complexed iron (as exemplified in Figure 1 top panel and quantified in bottom panel). We note that a 12-hour treatment with all 3 chelators markedly reduced the resident LIP of HepG2 cells (a change of 0.72 relative fluorescent units corresponds to an LIP of 1.2 μM according to the method described in Epsztejn et al[18] and reviewed in Esposito et al[20] and Kakhlon and Cabantchik[21]) (Figure 1D). However, an equivalent ½-hour treatment was highly effective with either DFP or ICL670 but marginally effective with DFO.

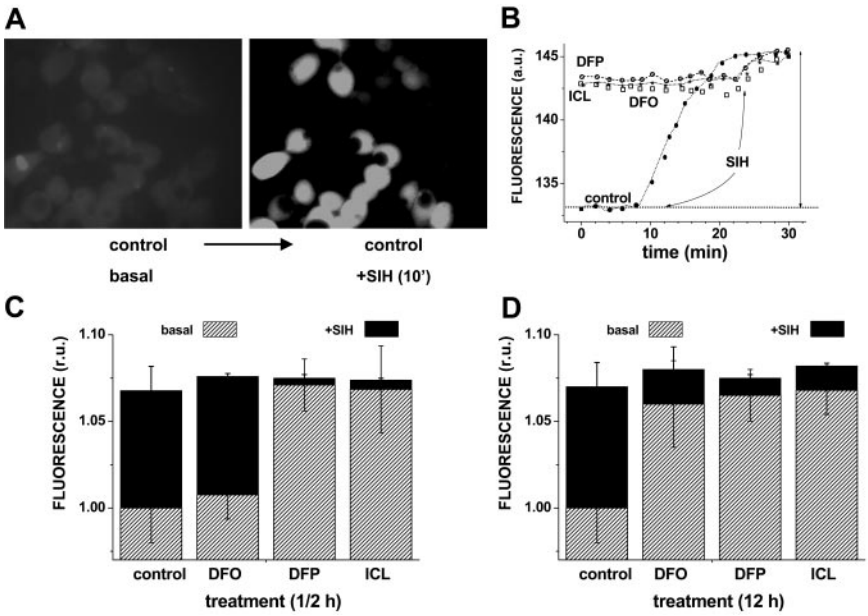

Figure 1. Effect of chelators on cytosolic LIP: time dependence of intracellular chelation of resident labile iron as analyzed in cells probed with the iron-sensitive CALB. HepG2 cells were preincubated for 0.5 hours (short term) or 12 hours (long term) with the indicated chelator (50 μM in growth medium), and prior to epifluorescence analysis (excitation, 385 nm; emission, 430 nm) they were loaded with CAL-B via its AM precursor. After washing with buffered saline, the cells were followed by epifluorescence microscopy under perfusion in DMEM–Hepes-buffered medium (with no phenol red) at 37°C. At the indicated times, the cells were supplemented with 50 μM SIH in order to obtain maximal recoverable fluorescence. (A) Snapshots of images of control cells preincubated 12 hours with no chelator (basal) and following a 10-minute treatment with SIH (in order to attain maximal recoverable fluorescence). (B) LIP analysis of cells treated for 12 hours with no chelator (control) or with the indicated chelator (50 μM). The fluorescence intensity values are mean values obtained at each time point from 5 different cells (in arbitrary units = a.u.); those corresponding to treatment prior to the addition of SIH (50 μM) denote the basal level of fluorescence. The solid vertical arrow represents the total fluorescence recovered in control cells by addition of SIH. The mean fluorescence intensity values are normalized to those associated with basal levels of control, and the difference between them and those attained by addition of SIH provides a measure for the cell chelatable iron, which we refer to as the labile iron pool (= LIP).[20] ● indicates control; ○, DFP; □, DFO; and *, ICL. The approach was applied to cells treated with chelators for either 12 hours (D) or 0.5 hours (C), with the slashed areas depicting the basal levels after 12-hour or 0.5-hour incubation and the black areas those attained with SIH (representing the residual LIP for each treatment). The bars depict standard errors of mean fluorescence intensity values obtained from 5 cells per field.

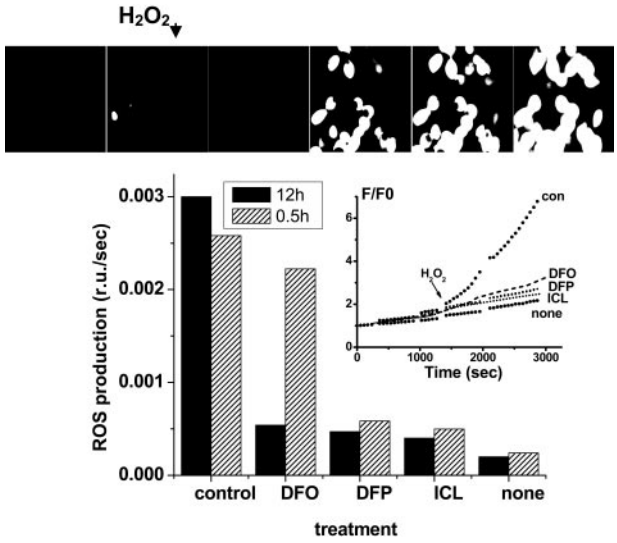

Figure 2. Effect of chelators on cytosolic LIP: time dependence of intracellular chelation of resident labile iron as analyzed in cells probed with the ROS-sensitive probe CDDHCF-DA. H9C2 cells were preincubated for either 0.5 or 12 hours with the indicated chelator (0 = control or 50 μM in growth medium), and prior to fluorescence analysis were loaded with the nonfluorescent oxidizable DCDHF (20 μM). After washing and resuspension in buffered saline supplemented with the same concentration of chelator, the systems were followed by epifluorescence microscopy (excitation, 485 nm; emission, 515 nm) under perfusion at 37°C, and H_2O_2 (35 μM) was added at the indicated time, except in the cases marked "none." The pictures (top) represent snapshots taken from control cells incubated with no chelator for 12 hours, and the inset represents the fluorescence tracings obtained with cells incubated with chelator for 12 hours (F/F0 is the fluorescence intensity of each experimental point normalized to the value at time zero). The bar graph provides the rates of fluorescence changes with time (= slopes calculated from the time courses shown in the inset given as relative fluorescence units F/F0 per second) for both 0.5- and 12-hour treatment with chelator.

The complementary assessment of residual LIP after chelation (approach A) is based on the determination of cell ROS production prompted by peroxides. Using the fluorogenic oxidizable CD-DHCF-DA probe, it can be determined that all chelators substantially reduced ROS formation in cells during the long (12 hours, 50 μM) incubation period. However, during the short incubation (0.5 hours, 50 μM), only the DFP and ICL were effective (Figure 2).

For online monitoring of chelator action in the cytosol, it was convenient to increase the LIP by loading the cells with permeant iron sources (eg, Fe(II) salts or Fe-hydroxyquinoline complexes [FeHQ]). The iron loading phase was also followed online by fluorescence microscopy using CALB-loaded cells (Figure 3) or by fluorescence intensity readings of CALG-loaded cells in a fluorescence plate reader (Figure 4A-B). Most of the CALG or CALB is targeted to the cytosol. After the incoming iron quenches significantly intracellular CALB fluorescence, further influx of iron is stopped by addition of the impermeant chelator DTPA in excess. Upon subsequent addition of ICL670, the intracellular fluorescence undergoes a time-dependent restoration, which increases with chelator concentration, indicating the chelator's cell-permeating and iron-chelating abilities (Figure 3).

The comparative efficacy of the 3 different chelators in accessing J774 cell overloaded with 2 different iron sources and chelating cytosolic iron are depicted in Figure 4A-B. The oral chelator DFP acted in a manner comparable with that of ICL670, whereas neither DFO (100 μM) nor DTPA (100 μM) elicited any significant effect on the LIP within 30 minutes. As the hydrophobic chelator SIH was found to be the fastest and most efficient chelator in restoring fluorescence in all cell systems studied,[31,32] we adopted it in all our experimental assays (at 50-100 μM) in order to generate the maximal dequenching level.[20]

In order to compare the intracellular chelating abilities of the different chelators in the 3 different cell types, we traced the fluorescence of CALG- and CALB-laden cells exposed to chelators in 96-well plates using a fluorescence plate reader. This high-throughput system enabled the follow-up of chelation kinetics in multiple samples (Figure 4C). Each experimental system was normalized to the initial fluorescence level, averaged, and plotted as depicted in Figure 4A-B for J774 cells. The probe-laden cells were initially exposed to a permeant iron salt or complex (FAS for Fe(II) or FeHQ for Fe(III)) in order to generate cytosolic iron–CALG complexes, as shown in Figure 4. Unlike DFO and DTPA, DFP and ICL were found to swiftly permeate into J774 cells and remove cytosolic iron complexed to CALG. Analogous results were found with DTPA, DFO, or ICL applied to CALB-loaded cells treated with FeHQ. The chelating properties of DFP could not be assessed in experiments using the quenching of CALB by FeHQ because of the propensity of HQ to form ternary complexes comprising CALB-FeHQ with affinities exceeding those of DFP (H.G. and Z.I.C., unpublished observations, August 2004). The

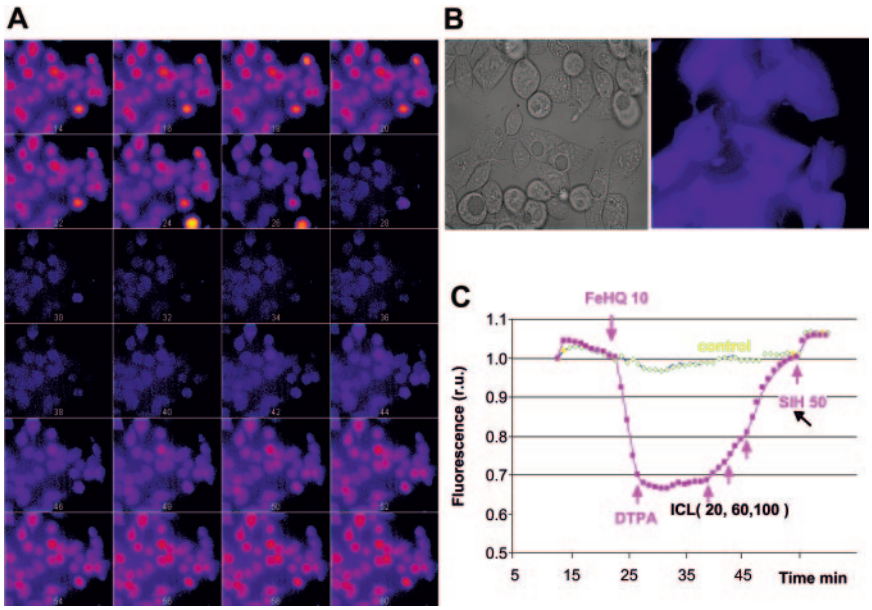

Figure 3. Online monitoring of intracellular chelation of resident and imposed LIPs. HepG2 cells labeled with CALB via its AM precursor (B, phase contrast and fluorescence) were followed by epifluorescence while perfused in media containing either HBS for up to 1 hour (control cells) or HBS containing the indicated substances added at the indicated times: Fe-HQ (1:1, 10 μM at 22 minutes), DTPA (100 μM at 27 minutes), ICL670 (added at 6-minute intervals from 38-minute time point to give final concentrations of 20, 60, and 100 μM), and SIH (100 μM at 55 minutes). All incubations and perfusions were carried out at 37°C. The montage gallery (A) depicts snapshots of the same field taken during the experiment, and the graph (C) depicts the average fluorescence density of 5 cells in each field (analyzed with NIH Image J [National Institutes of Health, Bethesda, MD]) and normalized to the initial fluorescence intensity (control cells and cells treated with ICL670 at the indicated μM concentration at the indicated time denoted with an arrow). Note: the montage gallery and the single pictures shown in panel B are based on different fields of cells.

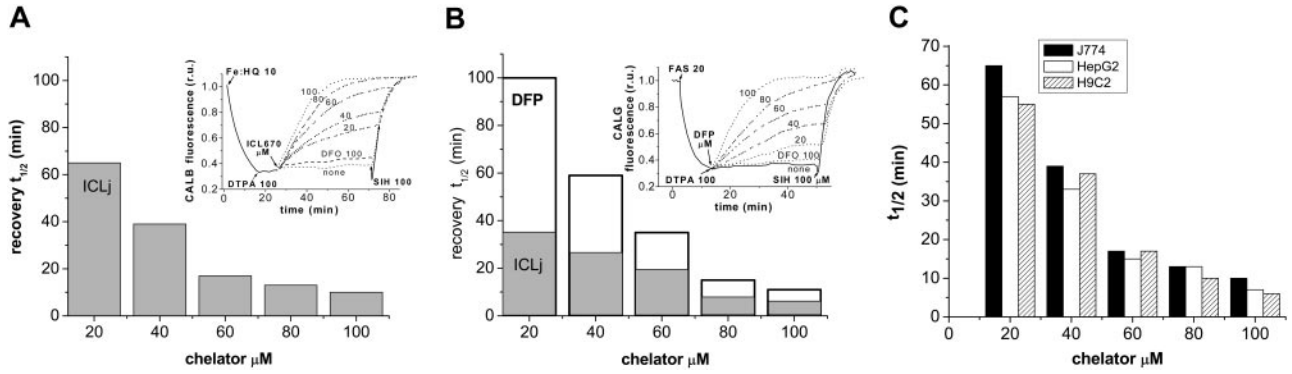

Figure 4. Intracellular chelation of iron with various chelators as monitored by fluorescence of J774 cells laden with CALG and CALB and quenched with externally added iron (online measurements). J774 cells labeled with either CALG (A) or CALB (B), loaded into the cytosol via their AM precursors as described in "Materials and methods," were exposed to either FAS 20 μM or FeHQ 10 μM for up to 10 minutes and subsequently to DTPA 100 μM for 2 to 5 minutes (to bind extracellular iron and stop further iron ingress) and to either none or the indicated concentration of chelator (in μM). At the end of the experiment, as indicated, all samples were also treated with 100 μM SIH. All incubations and perfusions were carried out at 37°C. The fluorescence measurements were carried out in a fluorescence plate reader with readings taken every minute. All experimental systems were run in triplicate, and the fluorescence intensity values were averaged and normalized to the initial fluorescence (insets). The half-time values of fluorescence recovery ($t_{1/2}$) for ICL obtained in FeHQ-loaded and FAS-loaded cells are given in panels A and B as a function of concentration (in μM) (gray areas), and those corresponding to DFP treatment are given in panel B superimposed on those of ICL treatment. (C) ICL670 comparative ability to chelate cytosolic labile iron pools in different cells (online measurements). The ability of ICL670 to access J774, H9C2, and HepG2 cells and chelate cytosolic iron was and is given in terms of half times ($t_{1/2}$) (minute) of CALB fluorescence recovery.

fluorescence recovery patterns evoked by each of the 3 chelators at relatively short time periods were similar in the 3 cell types studied. All data related to short exposures to pharmacologically relevant concentrations of chelators (20-100 μM) (Figure 4C) indicate that ICL670 and DFP (but not DFO) rapidly access the cytosol of 3 different cell lines and chelate their labile iron. However, in the long term, DFO attained similar effects to those of the other chelators.

Effect of chelators on endosomal iron

Iron loaded into endosomes by adsorptive endocytosis of CALG-Fe complexes was assessed as chelator-accessible iron in the 3 cell lines used in the present study (Figure 5). The full content of endosomal loaded iron was revealed by adding SIH, indicating that the system is amenable to chelation studies, similar to what has been shown above for cytosolic LIP. The J774 cells were most active in endocytosis, trailed by H9C2 and HepG2 cells. Endocytosis of the CALG-Fe complexes was detected when 1- to 2-hour incubations were carried out at 37°C but not at room temperature (not shown).

The accessibility of endosomal LIP to chelators was assessed in J774 cells loaded with CALG-Fe complexes via endocytosis (Figure 6A). We noticed that the basal fluorescence associated with CALG-laden endosomes drifted slightly upward with prolonged incubation times (> 30 minutes) at 37°C. The drift might indicate a small dissociation of the complex, which could be due to spontaneous release of iron due to the endosomal acidic pH and/or its transfer from endosome to cytosol. Figure 6A indicates that chelators such as ICL670, DFP, and also DFO were effective in chelating endosomal iron when applied at 37°C, but only DFP and ICL670 were effective when applied at 25°C, a temperature that strongly reduces endocytic activities. Since for up to an hour at 37°C DFO was differentially effective in accessing endosomal but not cytosolic iron, it can be implied that a major route of DFO entry into macrophage cells is via endocytosis, similar to what has been observed for CALG-Fe.

A virtually similar pattern of effects of chelators on CALG-Fe–laden endosomes was also obtained with HepG2 and H9C2 cells (not shown). However, in order to ascertain that hydrophilic chelators such as DFO can also gain access to cells via endocytosis, we applied the fluorescent-DFO analog in similar conditions as DFO and followed its intracellular localization after short- and long-term incubations. As seen in Figure 6B, J774 cells rapidly acquire the probe into their endosomes, a process that intensifies

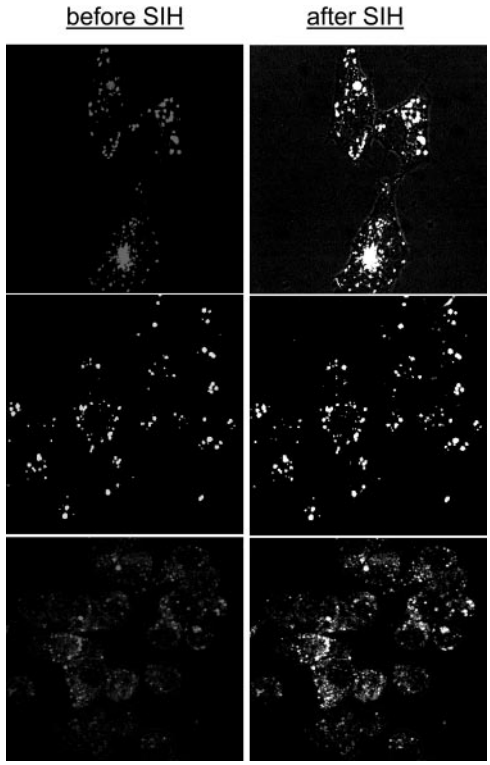

Figure 5. Chelation of endosomal labile iron generated by adsorptive endocytosis of CALG-Fe complexes in different cell types. HepG2 (top), H9C2 (middle), and J774 (bottom) cells were loaded with CALG-Fe complexes (50 μM) by incubating them in growth medium supplemented with 1% serum albumin. The depicted images represent overlays of images obtained before and after addition of 50 μM SIH (1-15 minutes, viewed by epifluorescence and merged with phase microscopy). All incubations and perfusions were carried out at 37°C. Probenecid (0.5 mM) was supplemented in order to minimize leakage of the calcein (CAL). The mean fluorescence intensity levels in the various cells following similar loading treatments and analyzed with equivalent parameters were (in relative terms) 10 for J774, 3 for H9C2, and 1 for HepG2.

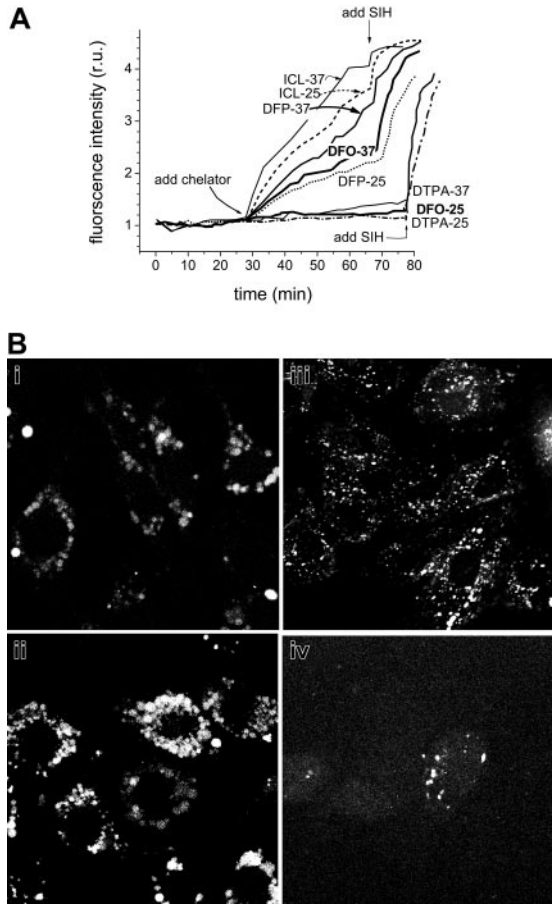

Figure 6. The effect of temperature on the recovery of fluorescence following addition of chelators in CALG-Fe–loaded endosomes of J774 cells. J774 cell endosomes were loaded under isotonic conditions with CALG-Fe (100 μM in DMEM for 20 minutes), then extensively washed with HBS medium containing 1% bovine serum albumin and perfused at either 37°C or 25°C with DMEM medium containing the indicated additives (100 μM chelators added as indicated) and probenecid (0.5 mM), which was supplemented in order to minimize leakage of the calcein. Images (epifluorescence) were taken at 1- to 2-minute intervals, and the average fluorescence intensity values of endosomes in 5 cells in a field were normalized to the corresponding one obtained at the onset of the treatment. (B) A fluorescent analog of DFO is taken up into endosomes of various cell lines. (i-ii) J774, (iii) H9C2, and (iv) HepG2 cells were incubated with 50 μM fluoresceinated DFO in growth medium for (i) 1 hour or (ii-iv) 12 hours, and after washing they were examined by LSM (fluorescein settings).

with increasing incubation times, while H9C2 and HepG2 cells do so similarly but at about one-third and one-ninth lower rates.

Effect of chelators on catalytically active iron in cytosol and mitochondria

The effect of chelators on the oxidation of the dihydro forms of dichlorocarboxyfluorescein and of rhodamine 123, which are converted to their fluorescent derivatives by intracellular ROSs, is depicted in Figure 7A,D. DHR (50 μM) was preincubated with H9C2 cells for 10 minutes in order to permit its accumulation in the mitochondria and monitoring by fluorescence microscopy. H_2O_2 (35 μM) was added to stimulate the catalytic generation of high levels of ROS by labile iron (Figure 7A-B). ICL670 and DFP (100 μM) effectively blocked the H_2O_2 prompted oxidation of DHR, while addition of 50 μM of the cleavable, permeant EDTA analog, BAPTA-AM, was ineffective. BAPTA failed to inhibit intramitochondrial DHR oxidation even when cells were preincubated with BAPTA-AM for 20 minutes in order to accumulate even higher levels of BAPTA in the cytosol (estimated intracellular concentrations attained were > 500 μM). We verified that sufficient BAPTA was present in the cells to chelate virtually all of the cytosolic labile iron detectable with CALG (not shown). This was corroborated by assessing the effect of chelators on CDDHCF-DA oxidation, which takes place primarily in the cytosol, as shown in Figure 2. ICL, DFP, and BAPTA-AM effectively blocked the ROS-induced oxidation of CDDHCF when applied shortly before or during the Fe exposure. DFO was marginally effective in the short term (1-2 hours) but similarly effective to the other chelators in the long term.

The ability of the various chelators to attenuate cytosolic ROS production was assessed comparatively in the 3 cell lines, essentially as described in Figure 2 microscopically but using a fluorescence plate reader (Figure 8). The effect of 200 μM ICL670 on ROS production was used as reference for maximal attainable inhibition by a permeant chelator. All 3 chelators were effective in reducing ROS production when incubated for an extended time period (18 hours). H9C2 and HepG2 cells were particularly chelator sensitive and the relative protection afforded was more than 80%. Similar results were obtained with J774 cells except that the chelator-sensitive component of ROS production was only 35%. However, when applied online, only DFP and ICL670 were immediately effective on the 3 cell lines, while DFO's effects were considerably slower and markedly weaker.

Discussion

Iron chelators are essential for the treatment of iron overload and useful as tools for understanding the roles of LIPs in iron metabolism. Although iron chelators have been used in the clinic and in the laboratory for a number of years and new formulations are in preclinical evaluation stages, little is known about the modes by which they gain access to cellular LIPs, chelate iron, and limit its involvement in ROS production. Understanding these modes is essential not only for assessing chelator efficacy, but also for designing agents with improved biomedical properties. The most accessible LIP in cells is assumed to be associated with the cytosol,[20,21] which, under normal conditions, represents the crossroads of cell iron movement regulated by a mechanism linked to iron sensing by iron-responsive proteins.[33,34] The cytosol is also the compartment where iron is released from heme by heme oxygenases and from where iron is sequestered into ferritin molecules. The cytosolic LIP has been shown to be composed of transitory iron (II) and (III) forms whose relative ratios are determined by the redox capacity of cells,[20,22] possibly mediated also by specific cell iron reductases.[35] The organellar LIPs comprise forms of iron that subserve different functions: in mitochondria they serve as sources for the formation of protein iron-sulfur clusters and porphyrins,[36] in endosomes they provide the source of iron derived from receptor-mediated endocytosis that translocates into the cytosol[37] or possibly also to mitochondria,[25] and in lysosomes they are apparently associated with products of iron protein degradation.[38]

The cellular LIPs expand in iron overload conditions and pose a threat to cell integrity, a phenomenon that iron chelators are theoretically designed to alleviate by gaining access to those pools and complexation of the metal as nonredox active forms. The novel oral chelators DFP and ICL670 were designed with that view in mind, namely as relatively small molecules with requisite partition coefficients that confer upon them high membrane permeation abilities and thereby also high cell iron extraction capacity. However, the fact that the relatively large, partially charged and hydrophilic chelator DFO shares none of those membrane permeation properties and yet has had a remarkable clinical success in

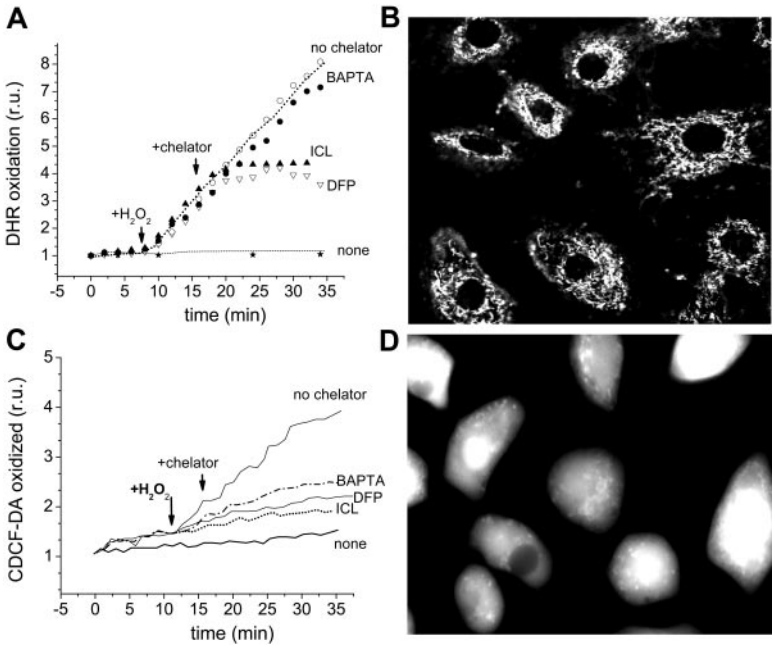

Figure 7. Effect of chelators on catalytically active iron in the cytosol and mitochondria of H9C2 cardiomyocytes. (A-B) Detection in mitochondria: The cells were loaded with DHR 50 μM (in HBS + 10 mM glucose) for 10 minutes at 37°C and washed, followed by epifluorescence (excitation, 488 nm; emission, 520 nm) at 1- to 2-minute intervals (A). After a baseline was established, agents were added at the indicated times: 35 μM H_2O_2, 100 μM chelator (ICL670 or DFP), or 50 μM BAPTA-AM . "None" indicates cells that received no treatment other than DHR, and "no chelator" refers to cells treated with H_2O_2 but with no chelator. (B) The image represents DHR-loaded cells treated with H_2O_2 but without chelator (fluorescence and phase merged). (C-D) Detection of oxidized CDCF in cytosol: The cells were preincubated with $FeSO_4$ for 1 hour at 37°C in HBS + 10 mM glucose, washed, resuspended in the same medium with no iron source but containing 20 μM CDDHCF-DA (the reduced precursor of CDCF), and examined by epifluorescence (excitation, 488 nm; emission, 520 nm) at 1- to 2-minute intervals (bottom left; fluorescence intensity given as relative units r.u.). Labels are as indicated for mitochondria, except that the images refer to CDDHCF-DA of cells prompted with Fe but treated with no chelator (fluorescence and phase merged) (D).

keeping iron overloaded patients in adequate iron balance indicates that membrane factors other than simple diffusion across the lipid bilayer might also contribute to the efficacy of chelation in living cells. Cells that are endowed with the capacity for adsorptive or fluid phase pinocytosis might acquire particular agents also by alternate routes of entry that differ from classical simple diffusion across membranes. Thus, chelators might access cellular labile iron pools not only according to their chemical character but also as determined by the unique membrane properties associated with particular cell types.

The present study represents an attempt to understand the mechanisms underlying chelator access to cellular sites of labile iron accumulation in model cell types relevant to iron overload, namely cells of hepatic, reticuloendothelial, and cardiac origin. We focused this study on representative cell lines that were found in preliminary studies to reproduce the properties of primary cultures of rat hepatocytes, rat neonatal cardiomyocytes, and human peripheral macrophages (G. Link, R.B.-E., and Z.I.C., unpublished observation, December 2004) in terms of accessibility to chelators such as DFP and DFO. The study deals with the most important agents presently available for clinical or preclinical use, DFO, DFP, and ICL670, along with the tridentate SIH,[31,32] which serves as a prototype of fast membrane-permeating and chelating agents.[20] Iron chelation was traced by following either the recovery of a fluorescence signal quenched by complexation of labile iron (LIP) to a fluorescent metallosensor or the inhibition of labile iron–mediated ROS formation.[20] The principle of chelation assessment at the level of cellular LIPs combined 2 complementary approaches: (1) monitoring the resident or residual LIPs in the cytosol, endosomes, and mitochondria of cells that were or were not previously treated with chelators and (2) monitoring online the LIPs generated in situ in cell organelles as Fe complexes (eg, CALG-Fe and CALB-Fe). Cytosolic targeting of metallosensors was accomplished by generating them within cells via permeation of their esterified precursor followed by their intracellular enzymatic hydrolysis. The traceable LIPs were derived either from endogenous labile iron sources or from supplemented permeant iron forms. We also targeted the complexes to the cytosol by hypertonic-isotonic loading following pinocytosis (H.G., R.B.-E., and Z.I.C., unpublished observations, December 2004). At the level of organelles, targeting of metallosensors to endosomes was based on the cellular ability to endocytose membrane-impermeant probes, whereas targeting to mitochondria relied on the probes' ability to accumulate in mitochondria driven by their membrane potential.

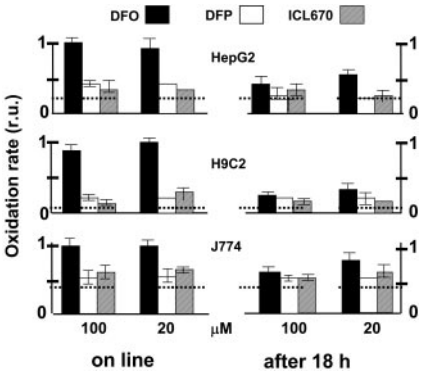

Figure 8. Comparative effects of chelators on cytosolic LIP as analyzed in various cell types probed with the ROS-sensitive oxidizable probe CDDHCF-DA. HepG2, J774, and H9C2 cells grown to confluence in 96-well culture plates were preincubated for 18 hours with the indicated chelator (0 = control, 20 or 100 μM in growth medium). Prior to fluorescence analysis, the cells were loaded with the nonfluorescent oxidizable CDDHCF-DA (10 μM), which generates the free acid intracellularly. After cells were washed and resuspended in buffered saline containing 10 mM glucose and 0.5 mM probenecid, fluorescence was followed in a fluorescence plate reader (excitation, 485 nm; emission, 515 nm) at 37°C: H_2O_2 (20 μM) (first) and chelator (second) were added sequentially (5-6 minutes apart). The slopes of fluorescence rise with time were calculated (as shown in Figure 2, inset) and are given relative (normalized) to the value of the control (no chelator added) ± SEM. "Online" comprises systems that were preincubated with no chelator, while "after 18 hours" comprises systems that were preincubated for 18 hours with the indicated chelator (0, 20, or 100 μM). The slopes of the respective controls (prior to normalization) were as follows for H9C2, HepG2, and J774 cells (in arbitrary fluorescence units/min): 980 ± 30, 425 ± 45, and 405 ± 33, respectively. The horizontal broken lines represent, for each cell type, the basal oxidation level that is not contributed by metal, revealed by addition of 200 μM ICL670.

Assessment of chelator action on cytosolic calcein-Fe labile complexes revealed that in the short term (up to 1 hour) the labile iron was readily chelated by the permeant DFP, ICL670, and SIH but not by the poorly membrane-permeant DFO (Figure 4A-B). These properties were observed in the 3 cell types used (Figure 4C), and they are in accord with the currently accepted view that only the small, partially lipophilic chelators can swiftly cross the plasma membrane and access cytosolic LIPs.[19,39] We also observed

that when offered to cells in serum-containing media, agents such as ICL670 and to a lesser extent DFP were slightly impeded in their ability to swiftly permeate into the cytosol and act on the cytosolic LIPs, apparently because of their avid adsorption to serum proteins (H.G., W. Breuer, and Z.I.C., unpublished observations, January 2005). This was also reflected in a reduction of ICL670's ability to prevent in vitro ROS formation in sera containing labile iron (H.G. and Z.I.C., unpublished observation, August 2004). Nevertheless, prolonged treatments (12-18 hours) with ICL670, DFP, or DFO were highly efficient in reducing the resident cytosolic LIP even in the presence of serum (Figures 1, 2, 8), indicating that endocytic uptake of chelators may be an important determinant of chelation in vivo. The fact that the highly hydrophilic species CALB and CALG, as free probes or as complexes with iron, or fluoresceinated DFO gained access to various cells via endosomes further supports the feasibility of the proposed auxiliary or primary mode of DFO entry into cells by endocytosis. Such a mechanism of DFO ingress might explain why this chelator is particularly efficient in removing iron from livers overloaded with iron in transfusional siderosis, where the major iron accumulation and its removal by DFO occurs in the actively endocytosing and phagocytosing Kupffer cells.[4]

The effect of chelators on iron complexes located in endosomes revealed properties of cell iron scavenging that might be important for understanding the mode of action of iron chelators as therapeutic agents and their relative advantages in particular cell types.[40] The small and lipophilic agents DFP, ICL670, and SIH were found to be effective in retrieving iron from endosomes in J774 cells at both room temperature and at 37°C, whereas DFO was effective only at 37°C (Figure 6A). The confinement of DFO's effects to the endosomal compartment and the high temperature coefficient of its action reinforce the above notion that the mode of DFO entry into cells encompasses highly temperature-dependent processes, unlike ICL670 or DFP. One likely mechanism by which this hydrophilic chelator could reach CALG-iron complexes enclosed within endosomes might be associated with endocytosis, followed by fusion of vesicles containing DFO with those containing CALG-Fe. Such a mechanism could also prevail for lipophilic chelators that, like ICL670, undergo major adsorption to plasma proteins, and yet have demonstrable effects on cellular LIPs, in accordance with the chelator's iron extracting capacity in vivo[14] but not with other in vitro studies.[41] Eventually, over a period of hours in culture conditions, the endosomal contents reach the cytosol and possibly also additional cell compartments by mechanisms that remain to be examined. Thus, lipophilic chelators seemingly act on both cytosolic and endosomal LIPs by virtue of their membrane permeation properties, per se, as well as by their incorporation into endocytic vesicles while bound to proteins. On the other hand, the cell chelating ability of hydrophilic chelators such as DFO would depend more on the endocytic ability of cells such as macrophages, hepatocytes, and cardiomyocytes (Figures 5-6). This ability is not restricted to cultured cell lines and was also observed with the same type of cells derived from neonatal rats and grown as primary cultures (R.B.-E. and Z.I.C, unpublished observation, January 2005). We may assume that in vivo iron chelators permeate into cells and sequester iron from the major cellular LIPs, so their efficacy in accessing and neutralizing those intracellular LIPs would differ according to their availability in plasma or interstitial fluids and their membrane-crossing ability. Likewise, the variable capacity to adsorptively endocytose particular substances, as in the case of macrophages, or to pinocytose medium, as in the case of cardiomyocytes and hepatocytes, could have a marked influence on the ability of chelators such as DFO to reach the LIPs. Moreover, such endocytotic mechanisms might also contribute to the cell delivery of hydrophobic chelators that, like ICL670, demonstrably adsorb to proteins such as albumin. An attempt to compare the modes and relative rates by which the various chelators access the cellular LIPs is depicted in Table 2.

Table 2. Mode and access rates of FMS ingress into cell compartments and chelation of labile iron

	Chelator					
	DFO		DFP		ICL670	
Compartment	D	E	D	E	D	E
Cytosol	–	+	+++	+	++++	+
Endosomes	–	+	++	+	+++	+
Mitochondria	–	–	+	–	+	–

The various chelators used in this study, deferrioxamine (DFO), deferriprone (DFP), and ICL670, are compared in terms of their modes and relative rates of access into model cells as determined by their capacity to bind labile iron (complexed to fluorescent probes) or reduce its involvement in ROS production. D and E indicate the access mode into the cell by diffusion or endocytosis, respectively.

– and + through ++++ denote a semiquantitative scale of the indicated property.

The action of chelators on mitochondrial LIP has been relatively more difficult to assess experimentally,[23,42,43] as the internal volume is relatively small and their surface-to-volume ratio large, so that they are highly susceptible to minor changes in iron content and other ionic manipulations. Targeting of fluorescent metallosensors to mitochondria has been accomplished in a manner analogous to that of other membrane potential sensitive probes.[23] However, the available metallosensing probes, which contain high-affinity chelating moieties, are not easily amenable to quantitative reversal of their iron complexes by pharmacologic or therapeutic concentrations of chelators. The approach used in this study to monitor mitochondrial labile iron was based on its capacity to generate ROSs when its levels are raised in cells and/or when its redox cycling capacity is prompted with pro-oxidants (Figure 7). Such capacity was assessed with the probe CDHCF-AM, which concentrates primarily in the cytosol, and the targeted probe DHR, a permeant cation whose passive accumulation in the mitochondria is driven by the strongly negative intramitochondrial potential. Both probes fluoresce when oxidized in a given compartment, and the involvement of iron in such oxidation events is discerned by its inhibition with chelators (Figure 7). As cytosolic CDDHCF oxidation is inhibited by relatively high concentrations of the cytosolic-generated chelator BAPTA, whereas the oxidation of the DHR in the mitochondria is not, it can be inferred that blockage of DHR oxidation by ICL670 or DFP results from direct chelation of mitochondrial LIP. However, experimental proof that chelators can directly affect the mitochondrial LIP[42,43] awaits the design of novel target-directed probes endowed with appropriate features for evaluating LIPs in small compartments. The development of novel iron sensors and tracing methodologies might assist also in elucidating mechanisms by which chelates formed in cells exit into the medium and are expelled from organisms. Initial attempts to address this question showed that DFO and its iron chelate are poorly permeant in neuroblastoma cells.[44] Similar studies have been done with DFP[19] but not with ICL670.

Acknowledgments

We thank Dr P. Ponka (Montreal) for generous supplies of SIH, N. Melamed-Book (Jerusalem) for advice with the LSM, and Drs W. Breuer and C. Hershko for advice and critically reading the paper.

References

1. Hershko C, Link G , Konijn AM, Cabantchik ZI. Iron chelation therapy. Curr Hematol. 2005;4:110-116.
2. Esposito BP, Breuer W, Sirankapracha P, Pootrakul P, Hershko C, Cabantchik ZI. Labile plasma iron in iron overload: redox activity and susceptibility to chelators. Blood. 2003;102:2670-2677.
3. Finch CA, Deubelbeiss K, Cook JD, et al. Ferrokinetics in man. Medicine (Baltimore). 1970;49:17-53.
4. Kushner JP, Porter JP, Olivieri NF. Secondary iron overload. Hematology (Am Soc Hematol Educ Program). 2001:47-61.
5. Olivieri NF, Brittenham GM. Iron-chelating therapy and the treatment of thalassemia. Blood. 1997;89:739-761.
6. Gabutti V, Borgna-Pignatti C. Clinical manifestations and therapy of transfusional haemosiderosis. Bailliere's Clin Haematology. 1994;7:919-940.
7. Borgna-Pignatti C, Rugolotto S, De Stefano P, et al. Survival and disease complications in thalassemia major. Ann N Y Acad Sci. 1998;850:227-231.
8. Olivieri NF, Nathan DG, MacMillan JH, et al. Survival in medically treated patients with homozygous β-thalassemia. N Eng J Med. 1994;331:574-578.
9. Modell B, Letsky EA, Flynn DM, et al. Survival and desferrioxamine in thalassaemia major. Brit Med J. 1982;284:1081-1084.
10. Davis BA, Porter JB. Results of long term iron chelation treatment with Deferoxamine. Adv Exp Med Biol. 2002;509:91-125.
11. Piga A, Gaglioti C, Fogliacco E, Tricta F. Comparative effects of deferiprone and deferoxamine on survival and cardiac disease in patients with thalassemia major: a retrospective analysis. Haematologica. 2003;88:489-496.
12. Hershko C, Cappellini MD, Galanello R, Piga A, Tognoni G, Masera G. Purging iron from the heart. Br J Haematol. 2003;125:545-551.
13. Liu ZD, Liu DY, Hider RC. Iron chelator chemistry. Adv Exp Med Biol. 2002;509:141-166.
14. Nick H, Acklin P, Lattmann R, et al. Development of tridentate iron chelators from desferrithiocin to ICL670. Curr Med Chem. 2003;10:1065-1076.
15. Hoyes KP, Porter JB. Subcellular distribution of desferrioxamine and hydroxypyridin-4-one chelators in K562 cells affects chelation of intracellular iron pools. Br J Haematol. 1993;85:393-400.
16. Cabantchik ZI, Kakhlon O, Epsztejn S, Zanninelli G, Breuer W. Intracellular and extracellular labile iron pools. Adv Exp Med Biol. 2002;509:55-75.
17. Jacobs A. An intracellular transit iron pool. Blood. 1977;50:4331-4336.
18. Epsztejn S, Kakhlon O, Glickstein H, Breuer W, Cabantchik ZI. Fluorescence analysis of the labile iron pool of mammalian cells. Anal Biochem. 1997;248:31-40.
19. Zanninelli G, Glickstein H, Breuer W, et al. Chelation and mobilization of cellular iron by different classes of chelators. Mol Pharmacol. 1997;51:842-852.
20. Esposito BP, Epsztejn S, Breuer W, Cabantchik ZI. A review of fluorescence methods for assessing labile iron in cells and biological fluids. Anal Biochem. 2002;304:1-18.
21. Kakhlon O, Cabantchik ZI. The labile iron pool: characterization, measurement, and participation in cellular processes (1). Free Radic Biol Med. 2002;33:1037-1046.
22. Petrat F, de Groot H, Sustmann R, Rauen U. The chelatable iron pool in living cells: a methodically defined quantity. Biol Chem. 2002;383:489-502.
23. Petrat F, Weisheit D, Lensen M, de Groot H, Sustmann R, Rauen U. Selective determination of mitochondrial chelatable iron in viable cells with a new fluorescent sensor. Biochem J. 2002;362:137-147.
24. Tsien RY. Fluorescent probes of cell signaling. Ann Rev Neurosci. 1989;12:227-253.
25. Zhang AS, Sheftel AD, Ponka P. Intracellular kinetics of iron in reticulocytes: evidence for endosome involvement in iron targeting to mitochondria. Blood. 2005;105:368-375.
26. Doulias PT, Christoforidis S, Brunk UT, Galaris D. Endosomal and lysosomal effects of desferrioxamine: protection of HeLa cells from hydrogen peroxide-induced DNA damage and induction of cell-cycle arrest. Free Radic Biol Med. 2004;35:719-728.
27. Burckhardt BC, Burckhardt G. Transport of organic anions across the basolateral membrane of proximal tubule cells. Rev Physiol Biochem Pharmacol. 2003;146:95-158.
28. Wrona M, Patel K, Wardman P. Reactivity of 2',7'-dichlorodihydrofluorescein and dihydrorhodamine 123 and their oxidized forms toward carbonate, nitrogen dioxide, and hydroxyl radicals. Free Radic Biol Med. 2005;38:262-270.
29. Sankaran NB, Banthia S, Samanta S. Fluorescence signalling of the transition metal ions: design strategy based on the choice of the fluorophore component. Proc Indian Acad Sci (Chem Sci). 2002;114:539-545.
30. Cabantchik ZI, Epstejn S, Breuer W. Novel methods for assessing transport of iron across biological membranes. In: Templeton DM, ed. Cellular and Molecular Iron Transport. New York, NY: Marcel Dekker. 2001:353-383.
31. Ponka P, Borova J, Neuwirth J, Fuchs O, Necas E. A study of intracellular iron metabolism using pyridoxal isonicotinoyl hydrazone and other synthetic chelating agents. Biochim Biophys Acta. 1979;586:278-297.
32. Richardson DR, Ponka P. Pyridoxal isonicotinoyl hydrazone and its analogs: potential orally effective iron-chelating agents for the treatment of iron overload disease. J Lab Clin Med. 1998;131:306-314.
33. Rouault T, Klausner R. Regulation of iron metabolism in eukaryotes. Curr Top Cell Regul. 1997;35:1-19.
34. Eisenstein RS. Iron regulatory proteins and the molecular control of mammalian iron metabolism. Ann Rev Nutrition. 2001;20:627-662.
35. Petrat F, Paluch S, Dogruoz E, et al. Reduction of Fe(III) ions complexed to physiological ligands by lipoyl dehydrogenase and other flavoenzymes in vitro: implications for an enzymatic reduction of Fe(III) ions of the labile iron pool. J Biol Chem. 2003;278:46403-46413.
36. Napier I, Ponka P, Richardson DR. Iron trafficking in the mitochondrion: novel pathways revealed by disease. Blood. Prepublished on November 4, 2004, as DOI 10.1182/blood-2004-10-3856. (Now available as Blood. 2005;105:1867-1874).
37. Breuer W, Epsztejn S, Cabantchik ZI. Iron acquired from transferrin by K562 cells is delivered into a cytoplasmic pool of chelatable iron(II). J Biol Chem. 1995;270:24209-24215.
38. Konijn AM, Glickstein H, Vaisman B, Meyron-Holtz EG, Slotki IN, Cabantchik ZI. The cellular labile iron pool and intracellular ferritin in K562 cells. Blood. 1999;94:2128-2134.
39. Cabantchik ZI, Glickstein H, Milgram P, Breuer W. A fluorescence assay for assessing chelation of intracellular iron in a membrane model system and in mammalian cells. Anal Biochem. 1996;233:221-227.
40. Cohen AR, Galanello R, Pennell DJ, Cunningham MJ, Vichinsky E. Thalassemia. Hematology (Am Soc Hematol Educ Program). 2004:14-34.
41. Hasinoff BB, Patel D, Wu X. The oral iron chelator ICL670A (deferasirox) does not protect myocytes against doxorubicin. Free Radic Biol Med. 2003;35:1469-1479.
42. Richardson DR, Mouralian C, Ponka P, Becker E. Development of potential iron chelators for the treatment of Friedreich's ataxia: ligands that mobilize mitochondrial iron. Biochim Biophys Acta. 2001;1536:133-140.
43. Richardson DR. Friedreich's ataxia: iron chelators that target the mitochondrion as a therapeutic strategy? Expert Opin Investig Drugs. 2003;12:235-245.
44. Richardson DR, Ponka P, Baker E. The effect of the iron(III) chelator, desferrioxamine, on iron and transferrin uptake by the human malignant melanoma cell. Cancer Res. 1994;54:685-689.